CrossMark

F–P interferometric cavity formed by two types of fiber Bragg gratings

Yu Meng[1,3] · Fu Gao[1] · Z. C. Zhuo[1] · Yan Pang[1] · Chao Chen[2] ·
Li Qin[2] · X. M. Su[1]

Abstract We proposed and demonstrated a new type of Fabry–Perot (F–P) interferometric cavity formed by a segment of bare fiber sandwiched by a dynamic grating in an Er^{3+} doped fiber and a fiber Bragg grating, in which the dynamic grating was formed in the section of Er^{3+} doped fiber by the forward-propagating probe field and its reflected component because of a high reflection fiber Bragg grating at the other end. An incoherent pump was applied to amplify the modulation amplitudes of the dynamic grating and therefore to control the output spectra of the F–P interferometric cavity. The transmitted spectra of the F–P interferometric cavity have been observed with different powers of the incoherent pump, which were accordance with the theoretical analyses. The scheme has potential applications in fiber-optic communication and fiber sensors.

1 Introduction

Dynamic Bragg gratings (DBG) in erbium-doped fiber (EDF) can be created by two counter-propagating coherent light waves with the resonate transition between the ground level ($^4I_{15/2}$) and the metastable level ($^4I_{13/2}$) of the erbium ions. The dynamic grating can

✉ X. M. Su
suxm@jlu.edu.cn

Z. C. Zhuo
zhuozc@jlu.edu.cn

1 Key Lab of Coherent Light, Atomic and Molecular Spectroscopy of Ministry of Education, College of Physics, Jilin University, Changchun 130012, People's Republic of China

2 Changchun Institute of Optics, Fine Mechanics and Physics, Chinese Academy of Sciences, Changchun 130033, People's Republic of China
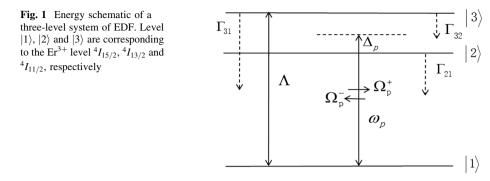
3 College of Optical and Electronical Information Changchun University of Science and Technology, Changchun 130012, People's Republic of China

be created by phase modulation for periodic change of fiber refractive index (Stepanov and Hernández 2007; Stepanov et al. 2007; Barmenkov et al. 2005). It also can be produced by amplitude modulation (Stepanov 2008; Melle et al. 2011) for a periodical variation of optic absorption (or gain) in space in a two-wave mixing (TWM) process (Hernandez et al. 2016). Here the physical essence for dynamic Bragg gratings are based on optical waves mixing processes which are different from that of the dynamic Brillouin grating. The dynamic Brillouin grating is resulted from three-wave interaction between one acoustic and two optical waves (Song et al. 2009, 2010). The acoustic wave can be separated from the stimulated scattering Brillouin process that happened in a birefringent medium such as a polarization-maintaining fiber. The earlier experimental demonstrations of dynamic gratings in EDF were reported by Frisken (1992) and Fischer et al. (1993). After that there have been many experiments to demonstrate DBG in EDF (Stepanov and Hernández 2007; Stepanov and Sánchez 2011). Later on, the DBGs in EDF are still extensively investigated for their important applications in single-frequency fiber lasing (Horowitz et al. 1994; Spirin et al. 2013), tunable narrow-band fiber filtering (Havstad et al. 1999; Xu et al. 2012), optical fiber sensors (Fan et al. 2005; Stepanov et al. 2009, 2016), adaptive interferometers (Stepanov et al. 2004; Rivera et al. 2013) and slow light (Stepanov and Sánchez 2009).

In the other hand, F–P cavities formed by a pair of fiber Bragg gratings (FBG) have been investigated recently (Guan et al. 2000; Ren et al. 2008). Comparing with a single fiber Bragg grating, this type of F–P cavity has narrower bandwidth of transmission (or reflection) spectra so that it has been applied in the fields of fiber optic sensing (Fan et al. 2012; Zhang et al. 2011) and optical communication (Town et al. 1995; Sun et al. 2006). However, it is hard to produce the F–P cavity (Qu et al. 2014) due to requirements for a pair of well-symmetrical gratings and shorter separation distance between the two gratings. Here, we proposed to use a dynamic grating to replace one of FBGs to create a new type of F–P interferometric cavity to overcome the shortcomings of the F–P cavity using the pair of FBGs. The dynamic grating can reach symmetrical to the FBG at the other end because it can be modulated dynamically by choosing appropriate parameters for erbium ions doped fibers, the pumping field, the probe field and FBG. The distance between DBG and FBG was several centimeters so that it was easily manufactured. Here a new type of dynamic grating is created to modulate both absorption of probe field and refractive index of erbium doped fiber with assistance of an incoherent pump. The modulating depth of the dynamic grating can be increased comparing with those without pumping because of amplified effect of the pump.

2 Theory

2.1 Reflection and transmission coefficient in DBG

A simplified three-level model of dynamic grating in EDF is shown as in Fig. 1, where levels $|1\rangle$, $|2\rangle$ and $|3\rangle$ are corresponding to the Er^{3+} level $^4I_{15/2}$, $^4I_{13/2}$ and $^4I_{11/2}$, respectively. Incoherent pump is resonant to the transition $|1\rangle \rightarrow |3\rangle$ whose pumping rate is Λ. The forward-propagating probe filed whose Rabi frequency Ω_p drives transition $|1\rangle \rightarrow |2\rangle$. The probe field and its reflected component (due to connection with a UV-written fiber Bragg grating in this scheme) create a standing wave field to induce periodic change of refractive-index and absorption (gain) of erbium doped fiber in propagating direction. This enable it dynamically tunable for transmission and reflection of the probe field.

In an interaction picture, the interaction Hamilton in the Hilbert space spanned by the bare states $|1\rangle$, $|2\rangle$ and $|3\rangle$ with rotational approximation is expressed as follows:

$$H_I = -\hbar[\Omega'_p|2\rangle\langle1|e^{-i\Delta_p t} + \Omega'^*_p|1\rangle\langle2|e^{i\Delta_p t}] \qquad (1)$$

where $\Delta_p = \omega_p - \omega_{21}$ is the frequency detuning between the frequency ω_p and resonant transition frequency ω_{21}, $\Omega'_p = 2\Omega_p \cos(k_p z)$ is Rabi frequency of standing-wave field and $\Omega_p = \mu_{21}E/2\hbar$ is the Rabi frequency of input probe field, μ_{21} is a dipole moment matrix element for the transition $|2\rangle \rightarrow |1\rangle$.

The response of the macroscopic medium to the field is governed by the density-matrix equation:

$$\frac{\partial \rho}{\partial t} = -\frac{i}{\hbar}[H_I, \rho] + \Gamma\rho \qquad (2)$$

where ρ stands for the density-matrix operator, and $\Gamma\rho$ represents all the effect caused by the interactions of Er^{3+} ion with fluctuations. We can define newly density-matrix elements:

$$\sigma_{21} = e^{i\Delta_p t}\rho_{21}, \ \sigma_{21} = \sigma^*_{12}, \ \sigma_{ii} = \rho_{ii} \qquad (3)$$

Inserting the above relations and Eq. (1) into (2), the equations of motion for the matrix elements are obtained as:

$$
\begin{aligned}
\dot{\sigma}_{21} &= (i\Delta_p - \gamma_{21})\sigma_{21} - i\Omega'_p(\sigma_{22} - \sigma_{11}), \\
\dot{\sigma}_{11} &= i\Omega'^*_p\sigma_{21} - i\Omega'_p\sigma_{12} + \Lambda(\sigma_{33} - \sigma_{11}) + \Gamma_{21}\sigma_{22} + \Gamma_{31}\sigma_{33}, \\
\dot{\sigma}_{22} &= i\Omega'_p\sigma_{12} - i\Omega'^*_p\sigma_{21} + \Gamma_{32}\sigma_{33} - \Gamma_{21}\sigma_{22}, \\
\sigma_{11} &+ \sigma_{22} + \sigma_{33} = 1
\end{aligned}
\qquad (4)
$$

where Γ_{ij} is spontaneous decay rate from level $|i\rangle$ to level $|j\rangle$. Here population decaying rates are chosen as $\Gamma_{31} = \Gamma_{21}$, $\Gamma_{32} = 10\Gamma_{21}$ in EDF (Zhuo et al. 2005). For $|2\rangle \rightarrow |1\rangle$ transition, $\Gamma_{21} = 1/\tau_{21}$, τ_{21} is lifetime of the metastable state $^4I_{13/2}$. The relaxation rate of non-diagonal element γ_{21} is related to the homogeneously broadened of transition from level $|2\rangle$ to level $|1\rangle$, which can be expressed as $\gamma_{21} = \Delta\omega/2$ (Desurvire 1990) and $\Delta\omega$ is full width of half maximum of the line. The pumping rate is $\Lambda = P_{pump}/\tau_{21}P^{th}_{pump}$, with P_{pump} and P^{th}_{pump} being the pump and threshold power (Desurvire 1990). The pumping rate is changeable when the power of the pump field is changed. The pump source at wavelength

of 980 nm has a broad bandwidth so as an incoherent field and therefore it cannot induce interference with medium and probe field but change the populations of the corresponding levels and therefore gain of probe field as shown in Eq. (4).

By solving Eq. (4) in the steady–state regime, we can obtain the density matrix element σ_{21} as:

$$\sigma_{21} = \frac{i(\gamma_{21} + i\Delta_p)(-\Gamma_{32}\Lambda + \Gamma_{21}(\Gamma_{31} + \Gamma_{32} + \Lambda))\Omega_p'}{\gamma_{21}^2(\Gamma_{32}\Lambda + \Gamma_{21}(\Gamma_{31} + \Gamma_{32} + 2\Lambda)) + \Delta_p^2(\Gamma_{32}\Lambda + \Gamma_{21}(\Gamma_{31} + \Gamma_{32} + 2\Lambda)) + 2\gamma_{21}(2\Gamma_{31} + 2\Gamma_{32} + 3\Lambda)\left|\Omega_p'\right|^2}$$

(5)

According to the definition of the polarization and susceptibility of the medium (Zhuo et al. 2005), the relevant susceptibility is obtained:

$$\chi(\Delta_p, z) = \frac{N_0 \mu_{21}^2 \sigma_{21}(\Delta_p, z)}{\varepsilon_0 \hbar \Omega_p'}$$

(6)

where N_0 is the ion density in EDF. The refractive index of the medium can be expressed as follows:

$$n(\Delta_p, z) = \sqrt{1 + \chi(\Delta_p, z)}$$

(7)

From Eq. (7), the refractive index $n(\Delta_p, z)$ is periodically modulated in space with the period $a = \lambda_p/2$ due to existence of the standing-wave field, λ_p is wavelength of probe field.

For the periodic medium, the method of transfer matrix is applied to obtain transmission and reflection of probe field. The whole medium includes many periods and and each period has the same transfer matrix due to the periodic modulation. For the length of the erbium-doped fiber L_1, the number of period is equal to $NN = L_1/a$, the total transfer matrix of the whole DBG (Su et al. 2014; Chen and Su 2013):

$$F_1 = \begin{pmatrix} M_{11} & M_{12} \\ M_{21} & M_{22} \end{pmatrix}^{NN}$$

(8)

where matrix M is the transfer matrix of every single period. It can be divided into many intervals and so

$$M = \prod M_1 M_2 \cdots M_j \cdots M_N$$

(9)

where N is the number of interval and for the jth interval

$$M_j = \frac{1}{t}\begin{bmatrix} t^2 - r^2 & r \\ -r & 1 \end{bmatrix}$$
$$= \frac{1}{4n}\begin{bmatrix} (n+1)^2 e^{ikdn} - (n-1)^2 e^{-ikdn} & (n^2-1)^2 e^{ikdn} - (n^2-1)^2 e^{-ikdn} \\ (n^2-1)^2 e^{-ikdn} - (n^2-1)^2 e^{+ikdn} & (n+1)^2 e^{-ikdn} - (n-1)^2 e^{ikdn} \end{bmatrix}.$$

(10)

The reflection and transmission coefficient of the probe field are $r_1 = F_{12}/F_{22}$ and $t_1 = 1/F_{22}$.

2.2 Reflection and transmission coefficient in a F–P cavity based on DBG and FBG

In the following, we derive the transfer matrix of the fiber F–P cavity. The fiber F–P cavity composes of three parts whose structure diagram shown in Fig. 2. The DBG recorded in erbium-doped fiber (the length L_1), a conventional FBG (the length L_2) and the interval part of bare fiber (cavity length L). The part of cavity length is non-exposed, and so the transfer matrix is:

$$F_2 = \begin{pmatrix} e^{-i\beta L} & 0 \\ 0 & e^{i\beta L} \end{pmatrix} \tag{11}$$

where β is propagation constant and $\beta = 2\pi n_0 / \lambda_p$

The transfer matrix of the FBG at the right-hand is obtained by using the coupled-mode theory (Li et al. 2001; Gafsi and El-Sherif 2000; Erdogan 1997):

$$F_3 = \begin{pmatrix} 1/t_2, & r_2^*/t_2^* \\ r_2/t_2, & 1/t_2^* \end{pmatrix} \tag{12}$$

where reflection and transmission coefficient are

$$r_2 = \frac{-\kappa \sinh(\sqrt{\kappa^2 - \sigma^2}L_2)}{\sigma \sinh(\sqrt{\kappa^2 - \sigma^2}L_2) + i\sqrt{\kappa^2 - \sigma^2}\cosh(\sqrt{\kappa^2 - \sigma^2}L_2)} \tag{13a}$$

$$t_2 = \frac{\sqrt{\kappa^2 - \sigma^2}}{\sqrt{\kappa^2 - \sigma^2}\cosh(\sqrt{\kappa^2 - \sigma^2}L_2) - i\sigma \sinh(\sqrt{\kappa^2 - \sigma^2}L_2)} \tag{13b}$$

where $\sigma = 2\pi n_{eff}\left(\frac{1}{\lambda_p} - \frac{1}{\lambda_B}\right)$ is a "frequency detunning parameter"; effective index $n_{eff} = n_0 + \delta n$, here n_0 is the core refractive index before the core was exposed, δn is the refractive index modulation depth; $\lambda_B = 2n_{eff}\Lambda_B$ is center wavelength of fiber Bragg grating, Λ_B is the grating period; $\kappa = \frac{\pi v}{\lambda_B}\delta n$ is a "mutual coupling coefficient" and here the fringe visibility of Bragg grating $v = 1$.

The transfer matrix of the whole F–P cavity is:

$$F = F_1 * F_2 * F_3 \tag{14}$$

Inserting Eqs. (8), (11) and (12) into Eq. (14), the reflection and transmission coefficient of F–P cavity are obtained:
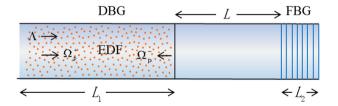

Fig. 2 Structure diagram of a fiber F–P cavity based on the DBG and FBG

$$t_{F-P} = \frac{t_1 t_2}{1 - r_1 r_2 e^{i2\beta L}} \tag{15a}$$

$$r_{F-P} = \frac{r_1/t_1 \cdot 1/t_2 \cdot e^{-i\beta L} + 1/t_1^* \cdot r_2/t_2 \cdot e^{i\beta L}}{1/t_1 \cdot 1/t_2 \cdot e^{-i\beta L} + r_1^*/t_1^* \cdot r_2/t_2 \cdot e^{i\beta L}} \tag{15b}$$

3 Results and discussion

3.1 The reflection characteristics of the DBG and the F–P cavity

In this section, we first discuss the characteristics of the DBG used for the generation of the F–P cavity. According to Eq. (9), the reflection spectra $R = |r|^2$ of probe field versus its wavelength λ_p in doped erbium fiber are drawn in different parameters of Rabi frequency Ω_p and pumping rate Λ. The selected EDF is Er110-4/125 of Thorlabs company. All the parameters are summarized in Table 1 (Desurvire et al. 1990). In order to exhibit the effect of incoherent pump on the DBG, reflection spectra are drawn without and with incoherent pumping field in Figs. 3 and 4, respectively.

In Fig. 3, we draw three groups of curves with different lengths of EDF and Rabi frequencies of the probe field without the incoherent pumping field. Parameters are chosen as: (a1) $\Omega_p = 1.0 \times 10^5 \Gamma_{21}, L_1 = 0.2$ m; (b1) $\Omega_p = 1.5 \times 10^5 \Gamma_{21}, L_1 = 0.2$ m; (c1) $\Omega_p = 2.0 \times 10^5 \Gamma_{21}, L_1 = 0.2$ m; (d1) $\Omega_p = 2.5 \times 10^5 \Gamma_{21}, L_1 = 0.2$ m; (a2) $\Omega_p = 1.0 \times 10^5 \Gamma_{21}, L_1 = 0.35$ m; (b2) $\Omega_p = 1.5 \times 10^5 \Gamma_{21}, L_1 = 0.35$ m; (c2) $\Omega_p = 2.0 \times 10^5 \Gamma_{21}, L_1 = 0.35$ m; (d2) $\Omega_p = 2.5 \times 10^5 \Gamma_{21}, L_1 = 0.35$ m; (a3) $\Omega_p = 1.5 \times 10^5 \Gamma_{21}, L_1 = 0.5$ m; (b3) $\Omega_p = 2.0 \times 10^5 \Gamma_{21}, L_1 = 0.5$ m; (c3) $\Omega_p = 2.5 \times 10^5 \Gamma_{21}, L_1 = 0.5$ m; (d3) $\Omega_p = 3.0 \times 10^5 \Gamma_{21}, L_1 = 0.5$ m. It is shown that the reflection of the probe field is increased with the power of probe field enhanced until the probe field is large enough to be saturated for a certain length of erbium fiber, or a certain optical density (Stepanov and Santiago 2006).

Table 1 Parameters used for DBG and F–P interferometric cavity

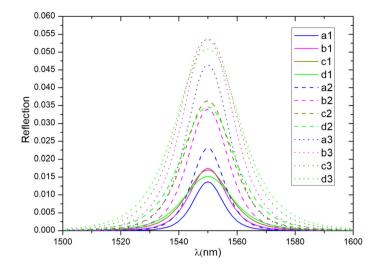| Symbol	parameter	value
Γ_{21}	Spontaneous decay rate for transition $|2\rangle \rightarrow |1\rangle$	100 Hz
$\Delta\omega$	Line-width at room temperature of homogeneously broadened for transition $|2\rangle \rightarrow |1\rangle$	9.26×10^{12} Hz[(Desurvire et al. 1990)]
ω_{21}	Resonance frequency for transition $|2\rangle \rightarrow |1\rangle$	$1.93548 \times 10^{14} \times 2\pi$ Hz
N_0	Erbium ion density	6.6×10^{25} m^{-3}
μ_{21}	Dipole moment matrix element for the transition $|2\rangle \rightarrow |1\rangle$	1.36×10^{-32} C m
L_1	Length of the EDF	0.35 m
L_2	Length of the FBG	0.007 m
L	Cavity length	0.04 m
λ_B	Bragg wavelength of FBG	1.55 μm
n_0	Fiber core refractive index	1.452
δn	Refractive index modulation depth of the FBG	3.0×10^{-4}
S_0	Fiber mode field diameter	4.5 μm

Fig. 3 Reflection spectra of probe field in DBG with different lengths of EDF and Rabi frequencies of the probe field under $\Lambda = 0$
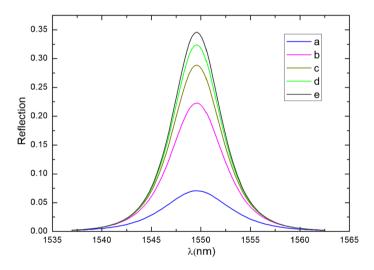

Fig. 4 Reflection spectra of the probe field in DBG with different pumping rates

The three groups of curves shows that the longer fiber has the larger saturated power of the probe field and therefore larger reflection can be achieved (Melle et al. 2011). The maximum modulated amplitudes of TWM process is proportion to optical density $\alpha_0 L_1$ (Stepanov and Santiago 2006), where α_0 is absorption coefficient. However, in experiment, a other factor to form a DBG is minimum power of probe field. A proper $\alpha_0 L_1$ needs smaller minimum power of probe field (Melle et al. 2011). We choose the length of the erbium fiber 0.35 cm in the following experiment of F–P cavity whose $\alpha_0 L_1 \approx 3.6$ and a small initial probe field is needed to generate a DBG as shown in Ref. (Melle et al. 2011). As the reflection of the DBG is too small to be below 0.1 under $\Lambda = 0$, we propose the scheme to enhance its reflection and therefore easily to fabricate F–P cavity (Li et al. 2001) with an

incoherent pumping. In Fig. 4, we draw a group of curves with different incoherent pumps with the same $\Omega_p = 1.5 \times 10^5 \Gamma_{21}$. Using the relationship between optical intensity and optical power (Boud 1992), Rabi frequency of $\Omega_p = 1.5 \times 10^5 \Gamma_{21}$ is corresponding to the power of probe field 0.8 mw. The pumping rate of the incoherent pumps are chosen as: (a) $\Lambda = 5\Gamma_{21}$; (b) $\Lambda = 15\Gamma_{21}$; (c) $\Lambda = 25\Gamma_{21}$; (d) $\Lambda = 35\Gamma_{21}$; (e) $\Lambda = 45\Gamma_{21}$. Form curves in Fig. 4, we find that the reflection of DBG has significantly increased comparing with those in the condition of $\Omega_p = 1.5 \times 10^5 \Gamma_{21}$. The reflection can gradually enhance with pumping rate increasing, but the reflection values increase less remarkable when pumping rate changes larger.

3.2 The transmission characteristics of the F–P cavity based on DBG and FBG

In the following, we first take simulation for the characteristics of the F–P cavity based on DBG and FBG and then observe them.

According to Eq. (14), we depict transmission spectra of the probe field in F–P cavity verses its wavelength in Fig. 5 with several pumping rates. The parameters used are Rabi frequency $\Omega_p = 1.5 \times 10^5 \Gamma_{21}$; pumping rates are $\Lambda = 0$, $0.5\Gamma_{21}$, Γ_{21}, $10\Gamma_{21}$ for curves Fig. 5a–d and other parameters are in Table 1. It is found that the transmission spectra of F–P cavity have two narrow peaks at edges of fiber Bragg gratings for all the curves in Fig. (5). The larger pumping rates result in narrower bandwidths of cavity. With the incoherent pumping rates increasing, the transmitted probe field at the edges is being increased for the reflected powers of probe fields are amplified. However inside bandgap of FBG, the modulation of F–P cavity is so small that it cannot be shown in the curves Fig. 5a–c until the incoherent pumping being strong enough it happens as shown in curve Fig. 5d. This exhibits that the dynamic F–P cavity is formed. On the other hand, the adverse periodic perturbation at two sides of transmission spectra of F–P cavity is resulting
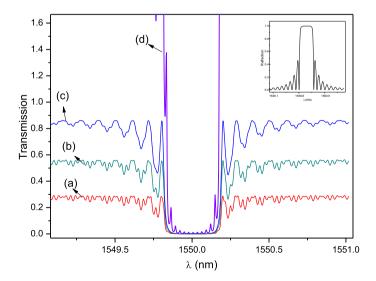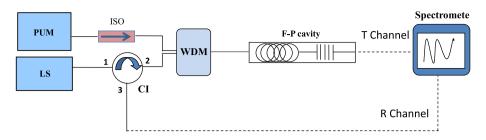

Fig. 5 Transmission spectra of the probe field in the F–P cavity based on DBG and FBG by using the same parameters in Fig. 4 and Table 1

Fig. 6 The setup diagram to observe transmission spectra of F–P cavity. *PUMP* incoherent pumping source at 980, *LS* light source at 1550 nm, *ISO* isolator, *CIR* circulators, *WDM* wavelength division multiplex, F–P cavity: the system formed by dynamic and UV-written Bragg gratings, *T Channel* transmission channel, *R Channel* reflection channel

from the impact of sidebands of FBG which is obvious as shown in reflection of probe field in the insert figure of Fig. 5. The spectra of the sidebands of FBG are disposed in making the FBG used in the experiment (see insert figure in Fig. 7).

In order to show the properties of the F–P cavity in Fig. (5), we carried out the experimental observation. The system of F–P cavity is made as mentioned in Fig. 5 with a 35 cm erbium fiber, a 3 cm bare fiber and 0.7 cm UW written FBG. The setup diagram was depicted in Fig. 6 where the incoherent pumping field and probe field are sources at 980 and 1550 nm. ISO was isolator for preventing reflection losses of pump and probe fields. The WDM is used as fiber coupler to mix the the 980 pumping and the 1550 light source together; F–P interferometric cavity was the system formed by dynamic and UV-written Bragg gratings; T Channel and R Channel are used for measurement of transmission and reflection spectra of FBG and F–P cavity. The measured transmission spectra of F–P cavity are shown in Fig. (7) with the power of the probe field is 0.2 mw and the powers of incoherent pumpings are 0, 50, 100 and 300 mw for curves Fig. 7a–d. The observation results are accordance with what shows in theoretical prediction above. Moreover, the
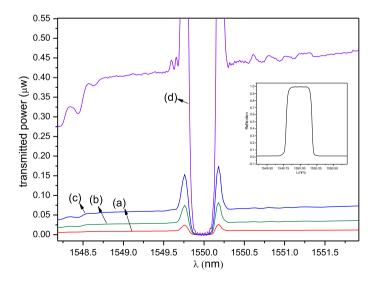

Fig. 7 Measured transmission spectra of the F–P cavity based on DBG and FBG under different powers of the incoherent pumping

negative impact of the sidebands of FBG is reduced since the sidebands of FBG in the F–P cavity is fabricated as designed in insert figure of Fig. 7.

4 Conclusion

In conclusion, we have proposed and demonstrated a scheme of F–P interferometric cavity by DBG in EDF and UV-written FBG. A three-level system of Er^{3+} is used to analyze the properties of the system with an incoherent pumping to amplify the modulation amplitude of the DBG and therefore the F–P cavity. The experimental observation was accordance with the theoretical analyses. This dynamic F–P cavity has potential applications in optical storage, and all-optical integrator and differentiator due to characteristics of narrower transmission spectra.

References

Barmenkov, Y.O., Kir'yanov, A.V., Andrés, M.V.: Time-domain distributed fiber sensor with 1 cm spatial resolution based on Brillouin dynamic grating. J. Quantum. Elect. **41**, 1176–1180 (2005)

Boud, R.W.: Nonlinear Optics, p. 432. Academic Press, London (1992)

Chen, Z.R., Su, X.M.: Asymmetrical spectra due to atomic coherence of neighboring excited levels. Eur. Phys. J. D **67**, 138–144 (2013)

Desurvire, E.: Study of the complex atomic susceptibility of erbium-doped fiber amplifiers. J. Lightw. Technol. **8**, 1517–1527 (1990)

Desurvire, E., Zyskind, J.L., Simpson, J.R., Photon, I.E.E.E.: Spectral gain hole-burning at 1.53 mu m in erbium-doped fiber amplifiers. Technol. Lett. **2**, 246–248 (1990)

Erdogan, T.: Fiber grating spectra. J. Lightw. Technol. **15**, 1277–1294 (1997)

Fan, X., He, Z., Hotate, K.: Novel distributed fiber-optic strain sensor by localizing dynamic grating in polarization-maintaining erbium-doped fiber: proposal and theoretical analysis. Jpn. J. Appl. Phys. **44**, 1101–1106 (2005)

Fan, L.J., Ma, L., Han, D.F., He, S.: Fiber bragg grating temperature sensor based on dynamic fabry-pérot cavity. Chin. J. Lasers **39**, 90–94 (2012)

Fischer, B., Zyskind, J.L., Sulhoff, J.W., DiGiovanni, D.J.: Nonlinear wave mixing and induced gratings in erbium-doped fiber amplifiers. Opt. Lett. **18**, 2108–2110 (1993)

Frisken, S.J.: Transient Bragg reflection gratings in erbium-doped fiber amplifiers. Opt. Lett. **17**, 1776–1778 (1992)

Gafsi, R., El-Sherif, M.A.: Analysis of induced-birefringence effects on fiber Bragg gratings. Opt. Fiber Technol. **6**, 299–323 (2000)

Guan, B.O., Yu, Y.L., Ge, C.F., Dong, X.Y.: Theoretical studies on transmission characteristics of fiber grating Fabry-Perot cavity. Acta Optica Sin. **20**, 34–38 (2000)

Havstad, S.A., Fischer, B., Willner, A.E., Wickham, M.G.: Loop-mirror filters based on saturable-gain or-absorber gratings. Opt. Lett. **24**, 1466–1468 (1999)

Hernandez, E., Stepanov, S., Sanchez, M.P.: Accelerated two-wave mixing response in erbium-doped fibers with saturable optical absorption. J. Opt. **18**, 085502 (2016)

Horowitz, M., Daisy, R., Fischer, B., Zyskind, J.: Narrow-linewidth, singlemode erbium-doped fibre laser with intracavity wave mixing in saturable absorber. Electron. Lett. **30**, 648–649 (1994)

Li, Y.F., Froggatt, M., Erdogan, T.: Volume current method for analysis of tilted fiber gratings. J. Lightw. Technol. **19**, 1580–1591 (2001)

Melle, S., Calderón, O.G., Zhuo, Z.C., Antón, M.A., Carreño, F.: Dynamic population gratings in highly doped erbium fibers. J. Opt. Soc. Am. B **28**, 1631–1637 (2011)

Qu, L., Meng, Y., Zhuo, Z.C., Guo, X.Z., Su, X.M.: Slow and fast light using fiber Bragg grating FP cavity. Optik **125**, 260–263 (2014)

Ren, W.H., Zheng, J.J., Wang, Y.H., Tao, P.L., Yan, F.P.: Theoretical analysis of the resonant characteristics of the Fabry-Perot cavity composed of fiber bragg grating. Acta Photonica Sin. **37**, 138–140 (2008)

Rivera, J.L., Sánchez, M.P., Miridonov, A., Stepanov, S.: Adaptive Sagnac interferometer with dynamic population grating in saturable rare-earth-doped fiber. Opt. Express **21**, 4280–4290 (2013)

Song, K.Y., Zou, W., He, Z., Hotate, K.: Optical time-domain measurement of Brillouin dynamic grating spectrum in a polarization-maintaining fiber. Opt. Lett. **34**, 1381–1383 (2009)

Song, K.Y., Chin, S., Primerov, N., Thévenaz, L.: Time-domain distributed fiber sensor with 1 cm spatial resolution based on Brillouin dynamic grating. J Lightwave technolggy **28**, 2062–2067 (2010)

Spirin, V.V., López-Mercado, C.A., Kinet, D., Mégret, P., Zolotovskiy, I.O., Fotiadi, A.A.: A single-longitudinal-mode Brillouin fiber laser passively stabilized at the pump resonance frequency with a dynamic population inversion grating. Laser Phys. Lett. **10**, 015102 (2013)

Stepanov, S.: Dynamic population gratings in rare-earth-doped optical fibres. J. Phys. D Appl. Phys. **41**, 224002 (2008)

Stepanov, S., Hernández, E.H.: Phase contribution to dynamic gratings recorded in Er-doped fiber with saturable absorption. Opt. Commun. **271**, 91–95 (2007a)

Stepanov, S., Hernández, E.H.: Detection of dynamic population gratings in erbium-doped optical fibers by means of transient fluorescence excited by oscillating interference pattern. J. Opt. Soc. Am. B **24**, 1262–1267 (2007b)

Stepanov, S., Sánchez, M.P.: Slow and fast light via two-wave mixing in erbium-doped fibers with saturable absorption. Phys. Rev. A **80**, 053830 (2009)

Stepanov, S., Sánchez, M.P.: Amplitude of the dynamic phase gratings in saturable Er-doped fibers. Appl. Phys. B **102**, 601–606 (2011)

Stepanov, S., Santiago, C.N.: Intensity dependence of the transient two-wave mixing by population grating in Er-doped fiber. Opt. Commun. **264**, 105–115 (2006)

Stepanov, S., Hernández, E., Plata, M.: Two-wave mixing by means of dynamic Bragg gratings recorded by saturation of absorption in erbium-doped fibers. Opt. Lett. **29**, 1327–1329 (2004)

Stepanov, S., Fotiadi, A.A., Mégret, P.: Effective recording of dynamic phase gratings in Yb-doped fibers with saturable absorption at 1064 nm. Opt. Express **15**, 8832–8837 (2007)

Stepanov, S., Cota, F.P., Quintero, A.N., Montero, P.R.: Population gratings in rare-earth doped fibers for adaptive detection of laser induced ultra-sound. J. Holography Speckle **5**, 303–309 (2009)

Stepanov, S., Sánchez, M.P., Hernández, E.H.: Noise in adaptive interferometric fiber sensor based on population dynamic grating in erbium-doped fiber. Appl. Optics **55**, 7324–7329 (2016)

Su, X.M., Sheng, J., Xiao, M.: Coupled atomic coherences induced by a standing wave. Opt. Commun. **318**, 120–127 (2014)

Sun, J.Q., Yuan, X.H., Zhang, X.L., Huang, D.X.: Single-longitudinal-mode fiber ring laser using fiber grating-based Fabry–Perot filters and variable saturable absorbers. Opt. Commun. **267**, 177–181 (2006)

Town, G.E., Sugden, K., Williams, J.A.R., Bennion, I.: Wide-band Fabry–Perot-like filters in optical fiber. IEEE Photonic Tech. L. **7**, 78–80 (1995)

Xu, P., Hu, Z.L., Jiang, N., Ma, L., Hu, Y.M.: Transient reflectance spectra of adaptive filters based on dynamic population gratings. Opt. Lett. **37**, 1992–1994 (2012)

Zhang, L., Wu, B., Ye, W., Shen, Y.H.: Highly sensitive fiber-optic vibration sensor based on frequency-locking of a FBG Fabry-Perot cavity. Acta Optica Sin. **31**, 88–92 (2011)

Zhuo, Z.C., Su, X.M., Zhang, Y.S.: Gain leveling using electromagnetically induced transparency. Phys. Lett. A **336**, 25–30 (2005)